α-Ketoacids Are Potent Slow Binding Inhibitors of the Hepatitis C Virus NS3 Protease

Frank Narjes,[‡] Mirko Brunetti,[§] Stefania Colarusso,[‡] Benjamin Gerlach,[‡,||] Uwe Koch,[⊥] Gabriella Biasiol,[§] Daniela Fattori,[‡] Raffaele De Francesco,[§] Victor G. Matassa,[‡] and Christian Steinkühler*[,§]

Departments of Biochemistry, Medicinal Chemistry, and Computational Chemistry, Istituto di Ricerche di Biologia Molecolare (IRBM) "P. Angeletti", Via Pontina Km 30 600, 00040 Pomezia, Italy

Received October 19, 1999; Revised Manuscript Received December 6, 1999

ABSTRACT: The replication of the hepatitis C virus (HCV), an important human pathogen, crucially depends on the proteolytic maturation of a large viral polyprotein precursor. The viral nonstructural protein 3 (NS3) harbors a serine protease domain that plays a pivotal role in this process, being responsible for four out of the five cleavage events that occur in the nonstructural region of the HCV polyprotein. We here show that hexapeptide, tetrapeptide, and tripeptide α-ketoacids are potent, slow binding inhibitors of this enzyme. Their mechanism of inhibition involves the rapid formation of a noncovalent collision complex in a diffusion-limited, electrostatically driven association reaction followed by a slow isomerization step resulting in a very tight complex. pH dependence experiments point to the protonated catalytic His 57 as an important determinant for formation of the collision complex. K_i values of the collision complexes vary between 3 nM and 18.5 μM and largely depend on contacts made by the peptide moiety of the inhibitors. Site-directed mutagenesis indicates that Lys 136 selectively participates in stabilization of the tight complex but not of the collision complex. A significant solvent isotope effect on the isomerization rate constant is suggestive of a chemical step being rate limiting for tight complex formation. The potency of these compounds is dominated by their slow dissociation rate constants, leading to complex half-lives of 11−48 h and overall K_i* values between 10 pM and 67 nM. The rate constants describing the formation and the dissociation of the tight complex are relatively independent of the peptide moiety and appear to predominantly reflect the intrinsic chemical reactivity of the ketoacid function.

The NS3 protein of the hepatitis C virus (HCV)[1] is a multifunctional polypeptide encompassing both an RNA helicase and a serine protease domain (*1*−*5*). The latter enzymatic function is responsible for proteolytic maturation of most of the nonstructural region of the viral polyprotein (reviewed in *6*). The hydrolytic activity of the NS3 protease is therefore thought to be absolutely required for the assembly of the viral replication machinery. Both enzymatic functions of the NS3 protein are presently the focus of intensive research since their inhibition is considered as a possible strategy for the development of antiviral pharmaceuticals (*7*, *8*).

To display its full proteolytic activity, the NS3 protease has to bind to the viral protein NS4A (*9*−*12*). In vitro, activation can be obtained by addition of synthetic peptides encompassing residues 21−34 of the NS4A cofactor to the purified enzyme (*13*−*18*). The X-ray crystal structures of the uncomplexed protease domain and of the binary serine protease−cofactor peptide complex have been determined (*1*−*3*). In addition, an NMR solution structure of the free enzyme has recently been obtained (*19*). Based on these structures, it was proposed that the cofactor activates the enzyme by stabilizing the fold of its N-terminal domain that contains residues involved both in catalysis and in substrate recognition (*19*).

The NS3 protease has an unusual substrate recognition mechanism. The minimum length of peptide substrates was shown to be a decamer spanning from P6 to P4′ (*20*−*22*). Specific recognition of substrate peptides is accomplished by the enzyme through a series of weak interactions that are distributed along a shallow, extended recognition surface. This natural predisposition of the NS3 protease for interacting with large substrate peptides, that will be difficult to develop into drug-like molecules, has driven the search for novel interactions that may allow anchoring of small molecules into the active site of the enzyme. It was recently shown that the NS3 protease undergoes a remarkable inhibition by its N-terminal cleavage products (*23*, *24*). This has subsequently allowed, using combinatorial techniques, generation of hexapeptide inhibitors with affinities in the low nanomolar

* To whom correspondence should be addressed at IRBM, Via Pontina Km 30 600, 00040 Pomezia, Italy. Phone: ++39 06 91093232; Fax: ++39 06 91093225; E-mail: Steinkuhler@IRBM.it.

[‡] Department of Medicinal Chemistry.

[§] Department of Biochemistry.

[||] Present address: R&D Chemistry, Biochemie GmbH, Biochemiestrasse 10, 6250 Kundl, Austria.

[⊥] Department of Computational Chemistry.

[1] Abbreviations: Cbz, benzyloxycarbonyl; Cha, cyclohexylalanine; CHAPS, 3-(3-cholamidopropyl)dimethylammonio-1-propanesulfonate; DABCYL, 4-[[4′-(dimethylamino)phenyl]azo]benzoic acid; Dap, diaminoproprionic acid; DTT, dithiothreitol; EDANS, 5-[(2′-aminoethyl)amino]naphthalenesulfonic acid; EDC, 1-ethyl-3′-(3-dimethylaminopropyl)carbodiimide hydrochloride; HATU, 2-(1-*H*-9-azabenzotriazol-1-yl)-1,1,3,3-tetramethyluronium hexfluorophosphate; HCV, hepatitis C virus; HOBT, *N*-hydroxybenzotriazole; HPLC, high-performance liquid chromatography; NS, nonstructural; p-APPA, *p*-amidinophenylpyruvate; PE, petroleum ether 40/60; RP, reversed phase; SIE, solvent isotope effect; TFA, trifluoroacetic acid.

10.1021/bi9924260 CCC: $19.00
Published on Web 01/29/2000

range (*25*). Binding of these inhibitors crucially requires two electrostatic interactions involving the P1 α-carboxylic acid function and an acidic residue in the P6 position (*25*−*27*). Attempts at decreasing the length of these molecules by removal of either P6 or P1 resulted in a substantial loss of potency (*25, 26*).

A viable strategy for finding small molecule inhibitors of the NS3 protease could take advantage of the intrinsic reactivity of its active site serine residue in developing mechanism-based inhibitors. A considerable amount of work has been published in the field of reversible, covalent inhibitors of serine proteases, and several classes of molecules have been identified and characterized in detail. Examples are aldehydes (*28, 29*), trifluoromethyl ketones (*30*−*33*), pentafluoroethyl ketones (*34*), ketoamides (*35*), boronic acids (*36*), and ketoacids (*37*−*39*). Aldehydes, ketoamides, trifluoromethyl ketones, and pentafluoroethyl ketones have in fact been described to be inhibitors of the NS3 protease as well (*40, 41*), with potencies ranging between 50 μM and 0.6 μM. The common mechanism of action of all these inhibitors is based on the presence of an electrophilic group capable of engaging in transient covalent bond formation with the γ-OH nucleophile of the catalytic serine residue, yielding a transition-state analogue of the tetrahedral intermediate that is normally formed during the cleavage reaction of amide or ester bonds. At variance with substrate molecules, this tetrahedral intermediate has an appreciable lifetime and will not further proceed through the transition state but revert back to yield the free enzyme and the regenerated inhibitor. The P1 residue preferred by the NS3 protease, cysteine, is chemically incompatible with the presence, within the same molecule, of an electrophilic group. We have recently found that difluoroaminobutyric acid, as a designed cysteine mimetic, is capable of replacing the native P1 residue in NS3 protease substrates and opens the way for the development of potent mechanism-based inhibitors of this enzyme (*42*).

In the present work, we present a detailed study on the mechanism of inhibition of the NS3 protease by peptide α-ketoacids incorporating difluoroaminobutyric acid in the P1 position. We show that these compounds are very potent, slow binding inhibitors of the proteolytic activity of NS3. A kinetic analysis reveals that this potency is mainly attributable to the formation of an extremely stable, reversible covalent complex.

MATERIALS AND METHODS

Synthesis. NMR spectra were obtained on a Bruker AMX 500 (500 MHz) or AMX 400 (400 MHz) spectrometer. Chemical shifts are reported in ppm from internal tetramethylsilane or the residual solvent peak. Data are reported as follows: chemical shift, multiplicity (s, singlet; d, doublet; t, triplet; q, quartet; qui, quintet; m, multiplet; b, broad), coupling constants, and integration. Low-resolution mass spectra (*m*/*z*) were recorded on a Perkin-Elmer API 100 (electrospray ionization) mass spectrometer; only molecular ions (M^+) are reported. Reversed phase analytical HPLC was performed on a Waters Symmetry C18 column (150 × 3.9 mm, 5 μm), flow rate 1 mL/min, using H_2O/0.1% TFA (A) and CH_3CN/0.1% TFA (B) as eluents; detection was at 220 nm with a Waters 996 PDA detector: gradient 1: linear, 90−0% A 10 min, then isocratic; gradient 2: linear, 70−40% A 10 min. Preparative HPLC was conducted on a Waters Symmetry C18 column (150 × 19 mm, 7 μm) or a Waters Prep Nova-Pak HR C18 cartridge (40 × 100 mm, 6 μm) using H_2O/0.1% TFA (A) and CH_3CN/0.1% TFA (B) as eluents; detection was at 220 nm with a Waters 486 absorbance detector. The synthesis of the inhibitors **1**−**5** was carried out as shown in Scheme 1. Complete experimental procedures for the synthesis of compounds **8**, **9**, **12**, and **14** necessary for their preparation can be found in reference *42*. Peptides **7**, **9**, **10**, **11**, and **13** were prepared using standard solution phase coupling protocols (*43, 44*).

Scheme 1[a]

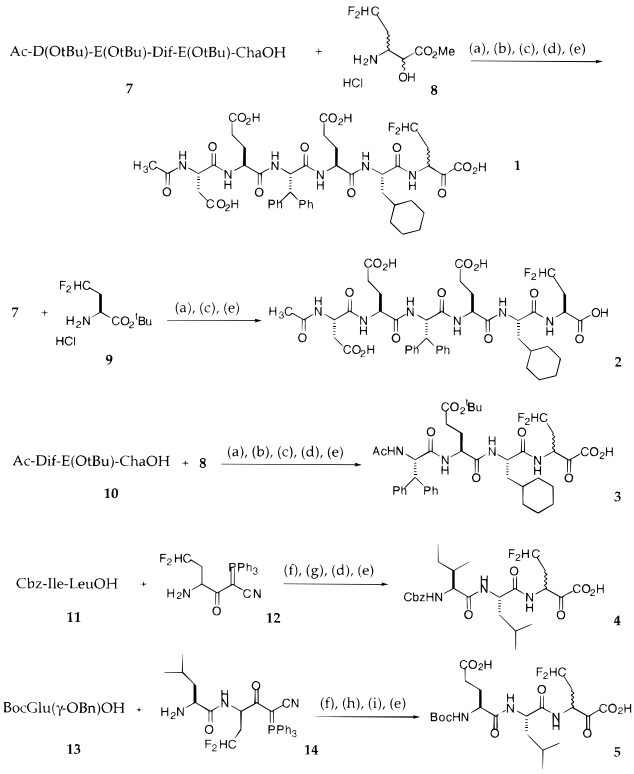

[a] Reagents: (a) HATU, 2,6-lutidine, DMF; (b) Dess-Martin periodinane, t-BuOH, CH_2Cl_2; (c) TFA, H_2O, CH_2Cl_2; (d) MeOH, 1 N NaOH; (e) RP-HPLC; (f) EDC, HOBt, CH_2Cl_2; (g) O_3, −78 °C, CH_2Cl_2/MeOH; (h) Pd/C, NH_4HCO_2; (i) O_3, −78 °C, CH_2Cl_2, THF, H_2O.

*Hexapeptide Ketoacid **1***. A 150 mg sample of pentapeptide AcD(OtBu)E(OtBu)DifE(OtBu)ChaOH (0.153 mmol), **7**, was dissolved in dimethylformamide (2 mL). HATU (64 mg, 0.17 mmol) and 2,6-lutidine (49 mg, 0.46 mmol) were added, and the solution was cooled to 0 °C. (±)-Methyl-3-amino-5,5-difluoro-2-hydroxypentanoate hydrochloride (40 mg, 0.18 mmol) (**8**) was added as a solid. The cooling bath was removed after 30 min and the resulting solution stirred overnight. The reaction was taken into a mixture of ethyl acetate and dichloromethane (150 mL, 3:1) and washed successively with 1 M aqueous $KHSO_4$ (3 × 80 mL), water (2 × 100 mL), and saturated aqueous $NaHCO_3$ and brine (2 × 100 mL). Drying (Na_2SO_4) and evaporation gave a solid, which was oxidized with Dess−Martin periodinane (195 mg, 0.46 mmol), in dichloromethane (3 mL) and *tert*-butyl alcohol (34 mg, 0.46 mmol). After stirring at room temperature for 24 h, ethyl acetate (50 mL) was added. The organic phase was washed 3 times with a mixture of aqueous saturated sodium hydrogen carbonate and aqueous saturated sodium thiosulfate (1:1, v/v), and then with brine. Drying

(Na_2SO_4) and evaporation gave a solid, which was deprotected with a solution of trifluoroacetic acid, dichloromethane, and water (50:45:5, v/v/v; 20 mL). After 30 min at room temperature, the solvents were evaporated in vacuo, and the remaining solid (158 mg) was dissolved in methanol (4 mL). Aqueous sodium hydroxide (1 mL, 1 N) was added and the solution left at room temperature for 15 min. Then aqueous hydrochloric acid (1 mL, 1 N) was added and the solution diluted with water/acetonitrile (70:30, v/v) and lyophilized. The product was isolated by preparative HPLC (Nova-Pak Prep): flow rate, 35 mL/min; gradient: linear, 75% A, 5 min isocratic, in 10 min to 50% A; 20 mg of crude per injection. First fraction: RT, 12.8 min, 50 mg (34%) of a colorless powder after lyophilization; 1 diastereomer, 99% pure by analytical HPLC (gradient 1, 6.9 min; gradient 2, 6.45 min). In the ^{1}H NMR, 15−20% of the ketoacid was hydrated. Addition of water gave a ratio of ketoacid to hydrate of 1:1. Only data for the ketoacid are reported. ^{1}H NMR (DMSO-d_6) δ 0.77−0.92 (m, 2 H), 1.05−1.43 (m, 6 H), 1.52−1.78 (m, 9 H), 1.82 (s, 3 H), 1.97−2.17 (m, 5 H), 2.30−2.50 (m, 3 H), 4.02−4.19 (m, 3 H), 4.37 (d, J = 10.3 Hz, 1 H), 4.49 (m, 1 H), 4.92 (m, 1 H), 5.21 (app. t, J = 9.3 Hz, 1 H), 6.08 (ddt, J = 3.3, 5.5, 56.0 Hz, 1 H), 7.03−7.38 (m, 10 H), 7.72 (d, J = 7.3 Hz, 1 H), 7.78 (d, J = 7.7 Hz, 1 H), 7.85 (d, J = 8.4 Hz, 1 H), 7.90 (d, J = 7.9 Hz, 1 H), 8.12 (d, J = 7.6 Hz, 1 H), 8.49 (d, J = 7.0 Hz, 1 H); MS *m*/z 959.9 (M^+ + H). Second fraction: RT: 13.9 min, 51 mg (34%), colorless powder after lyophilization; other diastereomer, 97% pure by analytical HPLC (gradient 1, 7.3 min). ^{1}H NMR (DMSO-d_6) δ 0.73−0.98 (m, 2 H), 1.05−1.50 (m, 6 H), 1.52−1.84 (m, 9 H), 1.84 (s, 3 H), 1.97−2.22 (m, 5 H), 2.30−2.50 (m, 3 H), 4.03−4.26 (m, 3 H), 4.39 (d, J = 10.2 Hz, 1 H), 4.49 (m, 1 H), 4.74 (m, 1 H), 5.21 (app. T, J = 9.2 Hz, 1 H), 6.06 (ddt, J = 3.6, 5.4, 56.4 Hz, 1 H), 7.03−7.38 (m, 10 H), 7.69 (d, J = 7.5 Hz, 1 H), 7.79 (d, J = 7.8 Hz, 1 H), 7.82 (d, J = 8.4 Hz, 1 H), 7.89 (d, J = 8.1 Hz, 1 H), 8.13 (d, J = 7.8 Hz, 1 H), 8.59 (d, J = 6.9 Hz, 1 H); MS *m*/z 959.6 (M^+ + H).

Compound ***2.*** Fifty milligrams of pentapetide AcD(OtBu)E(OtBu)DifE(OtBu)ChaOH (0.05 mmol) (**7**) was dissolved in DMF (0.5 mL) and cooled to 0 °C. HATU and solid (*S*)-*tert*-butyl-2-amino-4,4-difluorobutanoate hydrochloride (**9**) were added, followed by 2,6-lutidine (0.024 mL, 0.2 mmol). The reaction was allowed to reach room temperature and stirred for 3 h. Analytical HPLC (gradient 1) indicated incomplete conversion of the pentapeptide (∼30% remaining, RT 10.4 min, gradient 1, product 11.9 min). After another 2 h, the mixture was taken into ethyl acetate (100 mL) and washed successively with 1 N HCl (2 × 50 mL), saturated aqueous $NaHCO_3$ (2 × 50 mL), and brine. Drying with sodium sulfate and evaporation gave a light yellow solid, which was immediately deprotected with a solution of trifluoroacetic acid, dichloromethane, and water (60:30:10, v/v/v; 10 mL). After 30 min at room temperature, the solvents were evaporated in vacuo, and the remaining solid was separated by preparative HPLC (Waters Symmetry column): flow rate, 17 mL/min; gradient: linear, 68% A, 3 min isocratic, in 17 min to 65% A; 6 mg of crude per injection. The first peak was deprotected pentapetide (RT 11.6 min), the second the desired product compound **2** (RT 12.2 min); 11 mg (23%) of a colorless solid after lyophilization.^{1}H NMR (DMSO-d_6) δ 0.76−0.95 (m, 2 H), 1.08−1.32 (m, 4 H), 1.32−1.41 (m, 1 H), 1.42−1.51 (m, 1 H), 1.53−1.80 (m, 9 H), 1.83 (s, 3 H), 1.97−2.35 (m, 6 H), 2.38−2.50 (m, 2 H), 4.04−4.13 (m, 2 H), 4.13−4.21 (m, 1 H), 4.27−4.37 (m, 1 H), 4.38 (d, J = 10.3 Hz, 1 H), 4.47 (m, 1 H), 5.19 (app. t, J = 9.5 Hz, 1 H), 6.04 (ddt, J = 4.0, 5.7, 56.2 Hz, 1 H), 7.05−7.33 (m, 10 H), 7.75 (d, 1 H, J = 7.3 Hz, 1 H), 7.79 (d, 1 H, J = 8.0 Hz, 1 H), 7.89 (d, 1 H, J = 8.1 Hz, 1 H), 7.96 (d, 1 H, J = 7.6 Hz, 1 H), 8.10 (d, 1 H, J = 7.0 Hz, 1 H), 8.10−8.12 (bs, 1 H); MS *m*/z 929 (M^+ − H).

Compound ***3***. Two hundred milligrams of tripeptide AcDifE(OtBu)ChaOH (0.32 mmol), **10**, and HATU (129 mg, 0.34 mmol) were dissolved in dimethylformamide (2 mL), and the solution was cooled to 0 °C. Then 77 mg of **8** (0.35 mmol) in DMF (1 mL) and 2,6-lutidine (103 mg, 0.96 mmol) were added. The solution was allowed to reach room temperature and stirred overnight. The reaction was taken into ethyl acetate (60 mL) and washed successively with 1 M aqueous $KHSO_4$ (2 × 30 mL), and water, saturated aqueous $NaHCO_3$, and brine (2 × 30 mL each). Drying (Na_2SO_4) and evaporation gave 235 mg of a solid. Then 231 mg of this material was oxidized with Dess−Martin periodinane (374 mg, 0.88 mmol) in dichloromethane (2 mL) and *tert*-butyl alcohol (65 mg, 0.88 mmol). After stirring at room temperature for 3 h, analytical HPLC indicated complete conversion of the starting material. Ethyl acetate (100 mL) was added. The organic phase was washed 2 times with a mixture of aqueous saturated sodium hydrogen carbonate and aqueous saturated sodium thiosulfate (1:1, v/v, 50 mL), and then with brine. Drying (Na_2SO_4) and evaporation gave 220 mg of a colorless solid which was deprotected with a solution of trifluoroacetic acid, dichloromethane, and water (60:35:5, v/v/v; 20 mL). After 30 min at room temperature, the solvents were evaporated in vacuo to give a light yellow solid (221 mg). One hundred fifty milligrams of this material was dissolved in methanol (4 mL), and aqueous sodium hydroxide (1 mL, 1 N) was added. The solution was left at room temperature for 20 min. Then aqueous hydrochloric acid (1 mL, 1 N) was added and the solution diluted with water/acetonitrile (70:30, v/v, 15 mL) and lyophilized. The product was isolated by preparative HPLC (Nova-Pak Prep): flow rate, 30 mL/min; gradient: linear, 70% A, 5 min isocratic, in 13 min to 44% A; 10−12 mg of crude per injection. First fraction: RT: 13.6 min, 21 mg (14%) of a colorless powder after lyophilization; 1 diastereomer, 99% pure by analytical HPLC (gradient 1, 7.34 min; gradient 2, 7.72 min). In the ^{1}H NMR, 10−15% of the ketone was hydrated. Addition of water increased the ratio of ketoacid to hydrate to 1:1. Only data for the ketoacid are reported. ^{1}H NMR (DMSO-d_6) δ 0.73−0.91 (m, 2 H), 1.02−1.24 (m, 4 H), 1.24−1.43 (m, 2 H), 1.52−1.70 (m, 6 H), 1.65 (s, 3 H), 1.71−1.82 (m, 1 H), 1.96−2.08 (m, 2 H), 2.08−2.23 (m, 1 H), 2.28−2.40 (m, 1 H), 4.06 (m, 1 H), 4.15 (m, 1 H), 4.32 (d, J = 11.1 Hz, 1 H), 4.92 (m, 1 H), 5.22 (dd, J = 8.7, 11.1 Hz, 1 H), 6.08 (ddt, J = 3.6, 5.7, 55.9 Hz, 1 H), 7.04−7.32 (m, 10 H), 7.72 (d, J = 7.4 Hz, 1 H), 7.87 (d, J = 8.1 Hz, 1 H), 8.15 (d, J = 8.7 Hz, 1 H), 8.54 (d, J = 7.1 Hz, 1 H); MS *m*/z 715 (M^+ + H). Second fraction: RT: 14.8 min, 23 mg (15%), colorless powder after lyophilization; other diastereomer. ^{1}H NMR (DMSO-d_6) δ 0.74−0.93 (m, 2 H), 1.04−1.24 (m, 4 H), 1.24−1.43 (m, 2 H), 1.52−1.70 (m, 6 H), 1.65 (s, 3 H), 1.71−1.82 (m, 1 H), 1.96−2.08 (m, 2 H), 2.08−2.21 (m, 1 H), 2.28−2.39 (m, 1 H), 4.07 (m, 1 H),

4.16 (m, 1 H), 4.32 (d, J = 11.1 Hz, 1 H), 4.73 (m, 1 H), 5.21 (dd, J = 8.7, 11.1 Hz, 1 H), 6.06 (ddt, J = 3.6, 5.5, 56.4 Hz, 1 H), 7.04−7.32 (m, 10 H), 7.69 (d, J = 7.5 Hz, 1 H), 7.88 (d, J = 8.0 Hz, 1 H), 8.15 (d, J = 8.6 Hz, 1 H), 8.70 (d, J = 7.0 Hz, 1 H); MS *m/*z 715 ($M^+ + H$).

*Compound **4**.* The dipeptide Cbz-Ile-LeuOH (184 mg, 0.49 mmol), **11**, was dissolved in dichloromethane (4 mL), and EDC (102 mg, 0.54 mmol) and HOBt (72 mg, 0.54 mg) were added. The resulting solution was cooled to 0 °C, and (±)-4-amino-6,6-difluoro-3-oxo-2-triphenylphosphoranylidene-hexanenitrile (226 mg, 0.54 mmol) (**12**) was added in one portion. The ice bath was removed and the mixture stirred at room temperature for 90 min. The reaction mixture was diluted with ethyl acetate and washed successively with 1 N aqueous HCl, water, saturated aqueous $NaHCO_3$, and brine. Drying (Na_2SO_4) and evaporation gave a solid which was purified by flash chromatography (PE/ethyl acetate 1:2) to give 319 mg (83%) of Cbz-Ile-Leu-difluoro-3-oxo-2-triphenylphosphoranylidenehexanenitrile as a colorless powder (mixure of diastereomers, 2:1*). ^{1}H NMR (DMSO-d_6) δ 0.72−0.88 (m, 12 H), 1.04−1.15 (m, 1 H), 1.34−1.49 (m, 3 H), 1.52−1.63 (m, 1 H), 1.63−1.76 (m, 1 H), 2.00−2.22 (m, 1 H), 2.26−2.43 (m, 1 H), 3.88 (app. t, J = 8.1 Hz, 1 H), 4.30 (dd, J = 8.2, 14.6 Hz, 1 H), 4.36* (dd, J = 8.2, 15.6 Hz, 1 H), 4.92−5.10 (m, 3 H), 5.97, 5.99* (m, 1 H), 7.23−7.40 (m, 5 H), 7.51−7.68 (m, 12 H), 7.69−7.77 (m, 3 H), 7.89* (d, J = 8.5 Hz, 1 H), 7.94 (d, J = 8.0 Hz, 1 H), 8.07* (d, J = 7.9 Hz, 1 H), 8.18 (d, J = 7.9 Hz, 1 H). MS *m/*z 783 ($M^+ + H$). The foregoing compound (210 mg, 0.27 mmol) was dissolved in dichloromethane/methanol (6 mL, 7:3, v/v) and cooled to −78 °C. Ozone was bubbled through the solution until the blue color remained. The solution was then purged with nitrogen and stirred at room temperature for 2 h. Evaporation gave a light yellow oil, which purified by flash chromatography (PE/ethyl acetate 1:1) to yield 103 mg (68%) of a colorless solid, which was dissolved in methanol (3 mL). Aqueous sodium hydroxide (1 N, 1 mL) was added and the solution stirred at room temperature for 30 min. After addition of hydrochloric acid (1 N, 1 mL), the mixture was diluted with water/acetonitrile (80:20, v/v). The product was isolated by preparative RP-HPLC (Waters Symmetry): flow rate, 17 mL/min; gradient: linear, 80% A, 3 min isocratic, in 12 min to 40%. First fraction: RT: 12.2 min, 8 mg (8%) of a colorless powder after lyophilization; 1 diastereomer. ^{1}H NMR (DMSO-d_6) δ 0.75−0.91 (m, 12 H), 1.02−1.24 (m, 1 H), 1.34−1.47 (m, 3 H), 1.55−1.77 (m, 2 H), 2.02−2.20 (m, 1 H), 2.29−2.40 (m, 1 H), 3.89 (app. t, J = 8.2 Hz, 1 H), 4.28 (dd, J = 7.3, 15.4 Hz, 1 H), 4.93 (m, 1 H), 5.02 (d, J = 5.7 Hz, 2 H), 6.04 (tt, J = 3.2, 57.0 Hz, 1 H), 7.32−7.40 (m, 6 H), 7.96 (d, J = 7.6 Hz, 1 H), 8.44 (bs, 1 H). MS *m/*z 528 ($M^+ + H$). The second fraction contained a 1:1 mixture of the two diastereomers (34 mg, 34%).

*Compound **5**.* To a solution of BocGlu(OBn)OH (265 mg, 0.78 mmol), **13**, in dichloromethane (8 mL) were added EDC (158 mg, 0.82 mmol) and HOBt (137 mg, 0.9 mmol) at 0 °C. After 10 min, phosphoranylidene, **14** (400 mg, 0.747 mmol), was added as a solid. After stirring overnight, the reaction was worked up as described for compound **4**. Then 550 mg (0.64 mmol) of the crude product was dissolved in methanol (30 mL). Palladium on charcoal (1 g, 10% Pd) was added carefully, followed by ammonium formate (1.5 g). After TLC indicated complete conversion, the catalyst was removed by filtration and washed thoroughly with ethyl acetate. The filtrate was washed with water and brine. Drying over sodium sulfate and evaporation in vacuo gave an off-white solid (419 mg, 85%); 410 mg of this material was ozonized in dichloromethane (20 mL) at −78 °C. After the solution turned blue, ozonization was continued until TLC (PE/ethyl acetate 1:1) indicated complete consumption of the starting material. The ozone was removed by bubbling nitrogen through the reaction, and THF/water (4:1, v/v, 10 mL) was added. The cooling bath was removed and the mixture stirred at room temperature for 3 h. Evaporation gave a light yellow oil, which purified by medium-pressure chromatography (acetonitrile/water 3:7) using a RP C18 Lobar column (Fa. Merck KGA, Darmstadt) to yield 224 mg of a colorless powder after lyophilization. The product was isolated by preparative RP-HPLC (Waters Symmetry): flow rate, 17 mL/min; gradient: linear, 80% A, 3 min isocratic, in 12 min to 50%. First fraction: RT: 10.2 min, 40 mg (15%) of a colorless powder after lyophilization; 1 diastereomer. ^{1}H NMR (DMSO-d_6) δ 0.80−0.92 (m, 6 H), 1.37 (s, 9 H), 1.50−1.70 (m, 2 H), 1.55−1.72 (m, 1 H), 1.77−1.89 (m, 1 H), 2.10−2.24 (m, 1 H), 2.23 (m, 2 H), 2.30−2.42 (m, 1 H), 3.90 (m, 1 H), 4.27 (m, 1 H), 4.91 (m, 1 H), 6.04 (tt, J = 3.6, 56.8 Hz, 1 H), 6.93 (bs, 1 H), 7.84 (d, J = 7.5 Hz, 1 H), 8.60 (bs, 1 H). MS *m/*z 510 ($M^+ + H$). Second fraction: RT: 11.3 min, 50 mg (18%) of a colorless powder after lyophilization; other diastereomer. ^{1}H NMR (DMSO-d_6) δ 0.78−0.90 (m, 6 H), 1.37 (s, 9 H), 1.50−1.70 (m, 2 H), 1.55−1.72 (m, 1 H), 1.77−1.89 (m, 1 H), 2.10−2.24 (m, 1 H), 2.23 (m, 2 H), 2.30−2.42 (m, 1 H), 3.90 (m, 1 H), 4.27 (m, 1 H), 4.70 (m, 1 H), 6.03 (tt, J = 3.7, 57.2 Hz, 1 H), 6.94 (ds, J = 7.8 Hz, 1 H), 7.84 (d, J = 7.6 Hz, 1 H), 8.70 (bs, 1 H). MS *m/*z 510 ($M^+ + H$).

Enzyme Purification and Kinetic Assays. The NS3 protease domain from the HCV J strain encompassing amino acids 1027−1206 of the viral polyprotein as well as its K136M mutant was purified from *E. coli* as previously described (*45*). The catalytic serine mutant S139A was obtained in the context of the NS3 protease domain from the HCV Bk strain and purified as described in ref *20*. As protease cofactor, we used a synthetic peptide spanning the central hydrophobic core (residues 21−34) of the NS4A protein, containing a solubilizing lys-tag at its N-terminus [Pep4AK (KKKGSV-VIVGRIILSGR(NH_2)] (*17*). Activity assays were done in 50 mM Hepes, pH 7.5, 1% CHAPS, 1 mM DTT, 15% glycerol containing 80 μM Pep4AK using a synthetic substrate peptide corresponding to the NS4A/NS4B junction of the HCV polyprotein (Ac-DEMEECASHLPYK). An enzyme concentration of 10 nM was used in these experiments. Alternatively, an internally quenched fluorogenic depsipeptide substrate having the sequence Ac-DED(Edans)-EEAbuΨ[COO]ASK(Dabcyl)-NH_2 was used that allowed us to monitor the activity of an enzyme concentration of 0.2 nM (*46*). Reactions were performed at 23 °C, stopped by the addition of TFA, and analyzed by HPLC (*23*). IC_{50} values were determined at [S] = K_m as previously described (*47*). Progress curves were recorded using the fluorogenic depsipeptide substrate Ac-DED(Edans)EEAbuΨ[COO]ASK-(Dabcyl)-NH_2. To 0.5−1 nM NS3 protease in 50 mM Hepes, pH 7.5, were added 1% CHAPS, 1 mM DTT, 15% glycerol, 80 μM Pep4AK, and 10 μM substrate (5 × K_m) in the

absence or in the presence of increasing amounts of inhibitor. pH dependence experiments were done using a three-component buffer containing 25 mM Tris, 12.3 mM acetate, 12.3 mM Mes, 15% glycerol, 1% CHAPS, 1 mM DTT, and 80 μM Pep4AK. pH-dependent variations of ionic strength were corrected by addition of NaCl, such that the final ionic strength of all solutions was 25 mM. Spontaneous hydrolysis of the ester bond in the substrate at higher pH was negligible. Experiments were done in 1 mL cuvettes thermostated at 23 °C, using a circulating water bath, in a Perkin-Elmer LS50B fluorescence spectrometer. Fluorescence was excited at 355 nm, and emission at 495 nm was continuously recorded for up to 30 min. Excitation and emission slits were opened to 2.5 nm. Progress curves for inhibition of the NS3 protease were fitted by nonlinear least-squares analysis to the integrated expression eq 1 (*48*−*50*) using Kaleidagraph software:

$$F_{(t)} = V_f t + (V_0 - V_f)[1 - \exp(k_{obs} t)]/k_{obs} + F_i \quad (1)$$

where $F_{(t)}$ is the fluorescence at time t, V_f is the final steady-state velocity, V_0 is the initial velocity in the absence of inhibitor at $t = 0$, k_{obs} is the first-order rate constant for the approach to steady state, and F_i is the initial displacement of $F_{(t)}$ from zero at $t = 0$.

k_{obs} values were replotted as a function of inhibitor concentration and fitted with eq 2, assuming the validity of mechanism B in Scheme 1:

$$k_{obs} = k_{-2} + k_2\{I/[K_i(1 + (S/K_m) + I]\} \quad (2)$$

where k_2 and k_{-2} are rate constants describing the formation and dissociation of the final, tight EI* complex, respectively, and K_i is the dissociation constant of the initial EI complex. K_i values can further be obtained from the dependence of initial velocities on the inhibitor concentration. To this purpose, initial velocities V_0 obtained from the fit of the progress curve data to eq 1 were fitted with eq 3:

$$V_0 = V_{max} S/[K_m(1 + I/K_i) + S] \quad (3)$$

where V_{max} is the maximum velocity at substrate saturation and S and K_m are the concentration of the substrate and its Michaelis constant, respectively.

Protein fluorescence changes occurring upon addition of inhibitors to the NS3 protease were monitored using 100 nM enzyme in 50 mM Hepes, pH 7.5, 1% CHAPS, 1 mM DTT, 15% glycerol, and 80 μM Pep4AK. Fluorescence was excited at 280 nm, and emission at 330 nm was continuously recorded. The time-dependent fluorescence changes could be best fitted to a single-exponential equation. The observed pseudo-first-order rate constants obtained from this fitting procedure were plotted as a function of inhibitor concentration and used to calculate values for the second-order association rate constant from a fit to eq 4:

$$k_{obs} = k_{-2} + k_2[I/(K_i + I)] \quad (4)$$

The reaction leading to the EI complex was too fast to be monitored upon manual mixing. It was therefore followed on an SX-MV18 Applied Photophysics stopped flow instrument equipped with a fluorescence detector and interfaced with a Risc computer. The samples and the flow cell were thermostated at 23 °C using a circulating water bath. Two different techniques were used to determine association rate constants under these conditions. In a first approach, on-rates were determined by progress curve analysis, essentially as described above. Since the fluorogenic ester substrate used in this study shows burst kinetics (*21*), the sequential flow technique was chosen to selectively monitor the linear reaction phase dominated by the rate-limiting deacylation reaction. 20 nM NS3 protease in 50 mM Hepes, pH 7.5, 1% CHAPS, 1 mM DTT, 15% glycerol, 80 μM Pep4AK, and 10 μM substrate ($5 \times K_m$) was mixed in a first shot and preequilibrated in the aging loop of the instrument for 1 s before addition of the inhibitor in the second shot. The reaction was followed by monitoring the fluorescence emission >405 nm upon excitation at 355 nm. Progress curves thus obtained were fitted with eq 1 to derive values for k_{obs}. Plots of k_{obs} versus [I] were linear and fitted to eq 5 to obtain values for k_{on}:

$$k_{obs} = k_{on}[I]/[1 + ([S]/K_m)] + k_{off} \quad (5)$$

where [S] is the substrate concentration used in this experiment and K_m its Michaelis constant.

In a second approach, the time-course of displacement of the fluorescent active site probe Ac-D-E-Dap(*N*-β-dansyl)-E-Cha-C-OH (K_i = 200 nM) by added inhibitor was used to determine its association rate constant (*51*). To 400 nM NS3 protease in 50 mM Hepes, pH 7.5, 1% CHAPS, 1 mM DTT, 15% glycerol, 16 μM Pep4AK, and 7.3 μM probe were added increasing amounts of inhibitor. The time-dependent decrease of fluorescence emission at >405 nm, upon excitation at 280 nm, was monitored, and experimental data were fitted with a single-exponential equation to obtain values for k_{obs}. Association rate constants were obtained from a plot of k_{obs} versus [I] according to eq 6:

$$k_{obs} = k_{on}[I]/[1 + ([P]/K_d)] + k_{off} \quad (6)$$

where [P] is the concentration of probe and K_d its equilibrium dissociation constant. This equation holds only if probe dissociation does not become rate-limiting. The dissociation rate constant of P was previously determined to be 70 s^{-1} (*51*), indicating that pseudo-first-order rate constants significantly lower than this value can be accurately determined.

Dissociation rate constants of the tri- and tetrapeptide ketoacids were determined using the following procedure. The EI* complex was preformed by incubating 2 μM NS3 protease and 5−10 μM inhibitor for 1 h at 23 °C in 50 mM Hepes, pH 7.5, 1% CHAPS, 1 mM DTT, 15% glycerol, and 80 μM Pep4AK. The complex was then diluted 1000-fold into a buffer of the same composition containing 5 μM of the competitive inhibitor Ac-DEMEEC-OH (K_i = 0.6 μM), and activity recovery was monitored at timed intervals by adding 10 μM of substrate Ac-DED(Edans)EEAbuΨ[COO]-ASK(Dabcyl)-NH_2 to aliquots of the reaction mixture. The presence of the competitive inhibitor in the reaction mixture served a dual purpose. First, it prevented the reassociation of the ketoacid, trapping the free enzyme. In contrast to the ketoacids, Ac-DEMEEC-OH is in rapid equilibrium with the enzyme and can be readily displaced by added substrate. Second, it served the purpose of stabilizing the free enzyme. Since the dissociation kinetics of the ketoacids was very

slow, it had to be followed for more than 24 h, and under these conditions, a considerable decrease in the specific activity of control samples was noticed. Addition of the competitive inhibitor significantly stabilized the free enzyme, leading to less than a 15% decrease in specific activity over 65 h in control samples. The recovery of activity upon dissociation of tri- and tetrapeptide ketoacids was monophasic, and first-order rate constants were calculated from a fit of the recovery data to a single-exponential equation. Under these conditions, up to 70% of the enzymatic activity was recovered. The dissociation rate constant of the hexapeptide **1** which has a very low overall K_i* value, leading to significant inhibitor reassociation at longer incubation times even in the presence of added competitive inhibitors, could not be determined using this procedure. Extensive dialysis of diluted enzyme solutions, as an alternative method, could not be used due to enzyme instability in these conditions. In an alternative procedure, activity recovery was continuously monitored in a fluorescence cuvette upon dilution of the preformed EI* complex to a final concentration of 0.5 nM in 50 mM Hepes, pH 7.5, 1% CHAPS, 1 mM DTT, 15% glycerol, and 80 μM Pep4AK containing 20 μM substrate ($10 \times K_m$). The recovery of enzymatic activity was followed for up to 120 min. Under these conditions, only a small fraction of the EI* complex will dissociate, and reassociation is negligible. The first-order rate constants obtained for **3** and **4** from a fit of these data to eq 1, assuming 100% reversibility and monophasic kinetics, were in good agreement (less than 15% deviation) with the rate constants obtained from the analysis of longer experiments. This procedure was therefore used to give an estimate of the dissociation rate constant of compound **1**.

Solvent isotope effects (SIE) were determined in 50 mM Hepes, pD 7.9, 1% CHAPS, 1 mM DTT, 15% glycerol, and 80 μM Pep4AK in D_2O (99.9%, Sigma). This buffer was prepared as follows: 50 mM Hepes, 1% CHAPS, and 15% glycerol were prepared in D_2O. The solution was frozen, lyophilized, and redissolved in D_2O. This procedure was repeated 3 times in order to ensure the exchange of solute protons. To the final solution were added 1 mM DTT from a 1 M stock solution in D_2O and 80 μM Pep4AK from a 6.6 mM stock solution in D_2O, and the pD was determined from the pH-meter reading according to (*52*):

$$\text{pD} = (\text{pH-meter reading}) + 0.4 \qquad (7)$$

All manipulations were done under a constant flux of dry nitrogen. We estimate that the final buffer had an isotopic purity >99%. Kinetic data obtained in this buffer were compared to data obtained in H_2O solutions at pH = 7.5 and not at pH = pD in order to compare equivalent pL values (*52*), reflecting identical ionization states of the catalytic His 57 (*53*).

RESULTS

The α-ketoacid **1** (Scheme 1) incorporates previously obtained results on the structure−activity relationship (SAR) of hexapeptide inhibitors of the NS3 protease (*25*) as well as the designed, chemically inert, cysteine mimetic difluoroaminobutyric acid (*42*) as a replacement for the preferred natural cysteine P1 residue. **1** inhibited the NS3 protease with IC_{50} = 1 nM, a value 2 orders of magnitude lower than the one obtained with the homologous carboxylic acid **2** (*25*). From titration experiments performed under tight binding conditions, i.e., at an enzyme concentration 20 times higher than the IC_{50} value, we concluded that **1** formed a 1:1 complex with the enzyme that was devoid of catalytic activity (not shown). We found that the magnitude of IC_{50} values for **1** depended on the preincubation time, suggesting a slow-binding inhibition mechanism. This prompted us to investigate the interaction of **1** with the NS3 protease by progress curve analysis. Figure 1A shows a family of progress curves obtained upon simultaneous addition of a fluorogenic substrate together with increasing amounts of inhibitor. A time-dependent decrease in reaction rate on the minute time scale, consistent with the slow attainment of an equilibrium between enzyme, inhibitor, and substrate, was noticed. Slow-binding inhibition may result from any of the four mechanisms outlined in Scheme 2. In mechanism A, slow onset of inhibition results from an initial slow binding process. Alternatively, the rapid formation of a collision complex may be followed by a slow isomerization to a tight complex according to mechanism B. A third possibility, mechanism C, resides in a slow conformational equilibrium affecting the free enzyme with only one conformer binding to the inhibitor but not to the substrate. Alternatively, the inhibitor itself may undergo hydration−dehydration equilibria with only one species binding to the enzyme (mechanism D). Substantial hydration has been observed for a series of activated carbonyls in aqueous solution and was invoked as the origin of slow-binding inhibition of serine proteases by trifluoromethyl ketones (*32*). NMR spectra of the ketoacids used in the present study revealed that at pH 7.5 about 50% of the molecules were present as hydrates (data not shown). This value is much lower than those reported for aldehydes (*29*) or trifluoromethyl ketones (*32*), possibly reflecting the relatively low reactivity of the carbonyl moiety of α-ketoacids with respect to other activated carbonyls. Substantial hydration was therefore ruled out as the origin of slow-binding inhibition. The three mechanisms, A, B, and C, may be discerned by determining the dependence of the observed pseudo-first-order rate constant, k_{obs}, of formation of the enzyme−inhibitor complex on the inhibitor concentration. The resulting plots should be straight lines with positive slopes for mechanism A, display saturation in the case of mechanism B, and show a decrease of k_{obs} with increasing inhibitor concentration if mechanism C holds true. The progress curves shown in Figure 1A were fit with eq 1 to derive values for k_{obs}, and a replot of k_{obs} versus inhibitor concentration (Figure 1B) showed a hyperbolic increase in agreement with mechanism B. In fact, according to this mechanism, the formation of an initial EI complex that undergoes further isomerization will result in a linear increase of the pseudo-first-order rate constant k_{obs} at inhibitor concentrations below the K_i value of the initial EI complex. Once this complex is saturated, k_{obs} approaches the value of $k_2 + k_{-2}$, the sum of the first-order rate constants for the formation and dissociation of the tight EI* complex. Since these rate constants reflect intramolecular isomerizations, they will not depend on the inhibitor concentration. Accordingly, the data in Figure 1B contain the information both for the initial K_i value and for k_2 and k_{-2}. A fit with eq 2, that also takes into account the fractional occupancy of the enzyme by the substrate, gave K_i = 3 nM and $k_2 = 2.3 \times$

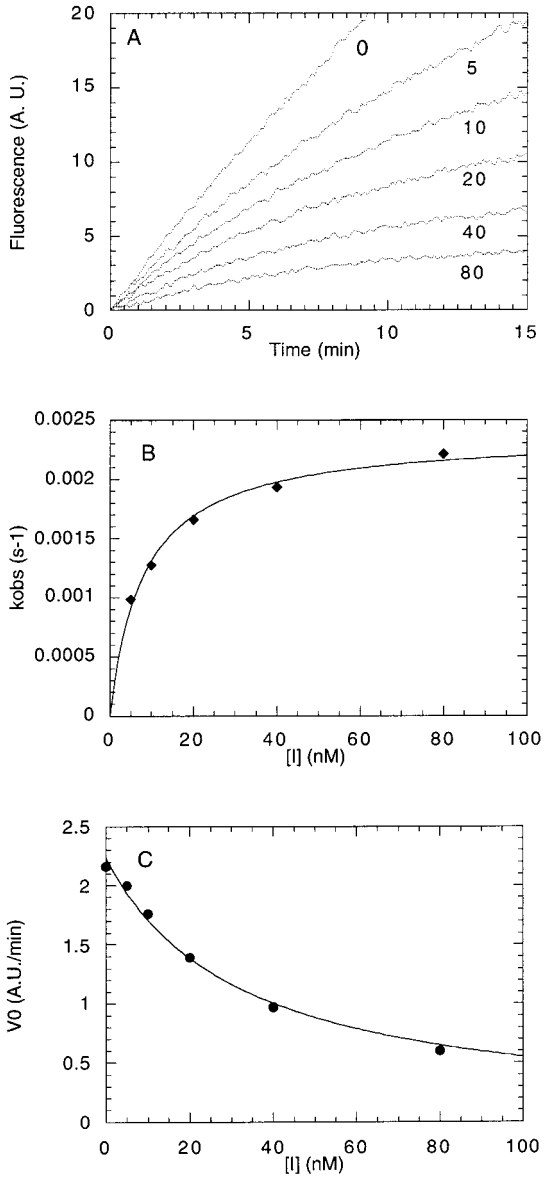

FIGURE 1: Progress curve analysis of the inhibition of the NS3 protease by the α-ketoacid **1**. To 0.5 nM NS3 protease in 50 mM Hepes, pH 7.5, were added 1% CHAPS, 1 mM DTT, 15% glycerol, 80 μM Pep4AK, and 10 μM ($5 \times K_m$) substrate Ac-DED(Edans)-EEAbuΨ[COO]ASK(Dabcyl)-NH_2. The cleavage reaction was continuously monitored by recording the fluorescence change at 495 nm upon excitation at 355 nm. Panel A: Progress curves obtained in the absence (0) or in the presence of the indicated nanomolar concentrations of **1**. Panel B: Data from panel A were fitted with eq 1 to derive values for the observed pseudo-first-order rate constant of formation of the enzyme−inhibitor complex, k_{obs}. These values were replotted as a function of inhibitor concentration. The line through the data represents a fit with eq 2 according to a biphasic inhibition model with a slow step ocurring in the second phase (mechanism B in Scheme 2). Since the *y*-axis intercept was too small to give an accurate value for k_{-2}, this rate constant was fixed at 5.7×10^{-6} s^{-1}, the experimentally determined off-rate, in the fit. Panel C: Initial velocities were calculated from a fit of the data in panel A with eq 1 and replotted as a function of inhibitor concentration. The line through the data represents a fit with eq 3.

10^{-3} s^{-1} (Figure 1B). The *y*-axis intercept turned out to be too small to give an accurate estimate for k_{-2}.

It can be noticed that the progress curves in Figure 1A do not have the same initial velocities. This results from the formation of the initial EI complex within the dead time of manual mixing. Initial velocities can be derived from the fit

Scheme 2

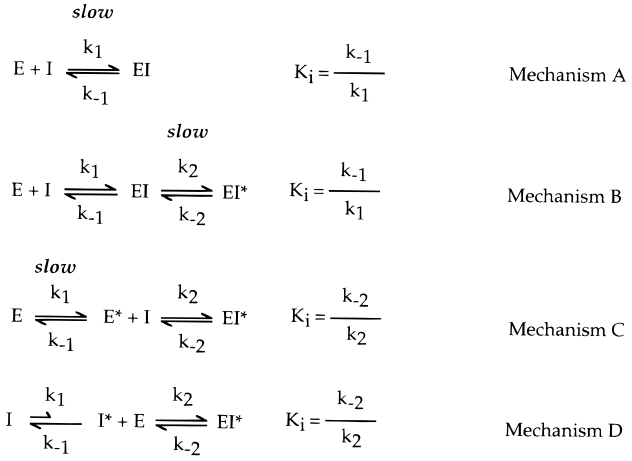

with eq 1 and contain the information for K_i. Figure 1C shows a plot of initial velocity as a function of [I]. Equation 3 was used to fit the data, yielding $K_i = 5$ nM, which is similar to the K_i value calculated from the plot in Figure 1B.

The assignment of values for K_i and k_2 from the previous experiment is based on the assumption of rapid equilibrium, i.e., that $k_2 \ll k_{-1}$ (*54*). This was verified by analyzing the reactions leading to formation of the EI complex on the millisecond time scale using a stopped-flow instrument. k_{obs} values were determined by the addition of increasing amounts of inhibitor in the presence of a fixed amount of fluorogenic substrate or by following the kinetics of displacement of the fluorescent active site probe P. Plots of k_{obs} versus inhibitor concentration were linear in both experimental settings (Figure 2A,B), allowing the calculation of the second-order rate constant k_1 for the formation of the initial EI complex by fitting the experimental data with eqs 5 and 6. We obtained values of 5.6×10^7 M^{-1} s^{-1} (Figure 2A) and 7.4×10^7 M^{-1} s^{-1} (Figure 2B), respectively. From these values for k_1, k_{-1} can be calculated from the known K_i value according to $k_{-1} = K_i k_1$. We obtained $k_{-1} = 0.16-0.22$ s^{-1}. These values are 2 orders of magnitude higher than k_2. This justifies the rapid equilibrium assumption.

The kinetics of inhibition of the NS3 protease by the tetrapeptide α-ketoacid **3** and the tripeptide α-ketoacids **4** and **5** (Scheme 1) were next determined by progress curve analysis. Table 1 summarizes the results, showing that a decrease of the peptide length went along with a substantial increase in K_i values but had little effect on the isomerization rate constant k_2. The pseudo-first-order rate constants for the formation of the initial EI complexes with the tri- and tetrapeptides were too fast to be accurately measured by stopped-flow. In fact, the association process of 5 μM of tetrapeptide **3** occurred with a half-life of less than 5 ms. This implies that k_{obs} for this process is larger than 138 s^{-1}. From $k_{obs} = k_{-1} + k_1[I]$, $k_{-1} = K_i k_1$, and $K_i = 4.6$ μM (Table 1), a lower limit for the association rate constant on the order of 10^7 M^{-1} s^{-1} can be estimated, indicating that a decrease in peptide length primarily affects k_{-1}.

We noticed that incubation of the NS3 protease with α-ketoacids **1**, **3**, and **4** resulted in a time-dependent increase in protein fluorescence (data for **4** are shown in Figure 3A). This increase could be best fit with a monophasic exponential curve. k_{obs} values, derived from this fit, were determined at

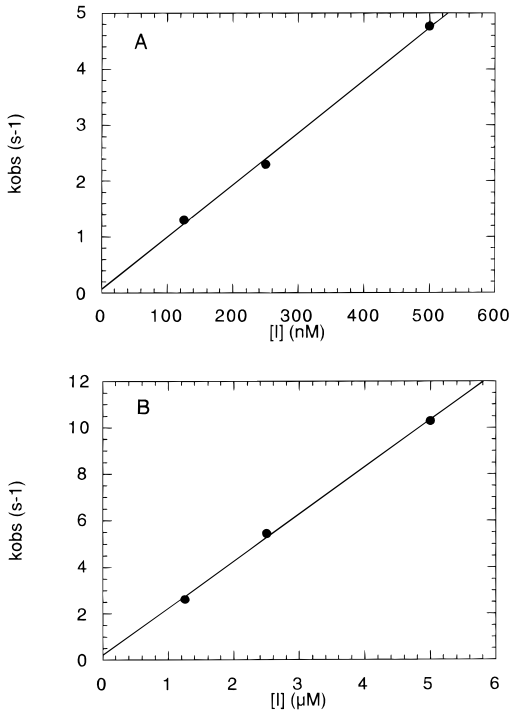

FIGURE 2: Analysis of the fast phase of enzyme−inhibitor complex formation by stopped flow. Panel A: 20 nM NS3 protease in 50 mM Hepes, pH 7.5, 1% CHAPS, 1 mM DTT, 15% glycerol, 80 μM Pep4AK, and 10 μM substrate (5 × K_m) Ac-DED(Edans)-EEAbuΨ[COO]ASK(Dabcyl)-NH_2 was preequilibrated for 1 s prior to addition of increasing amounts of **1**. The reaction was followed by monitoring the fluorescence emission >405 nm upon excitation at 355 nm using an appropriate cutoff filter. Progress curves thus obtained were fitted with eq 1 to derive values for the pseudo-first-order rate constant of formation of the enzyme−inhibitor complex, k_{obs}. k_{obs} values were subsequently plotted as a function of inhibitor concentration. The line through the data represents a fit to eq 5 from which the second-order association rate constant k_{on} was calculated. Panel B: To 400 nM NS3 protease in 50 mM Hepes, pH 7.5, 1% CHAPS, 1 mM DTT, 15% glycerol, 16 μM Pep4AK, and 7.3 μM of the fluorescent active site probe Ac-D-E-Dap(*N*-β-dansyl)-E-Cha-C-OH were added increasing amounts of inhibitor **1**. The time-dependent decrease of fluorescence emission at >405 nm, upon excitation at 280 nm, resulting from the displacement of the probe by the inhibitor was monitored. Experimental data were best fitted with the single-exponential equation: $F = F_f + A \exp(-k_{obs}t)$, that describes the decrease of the initial fluorescence $A + F_f$ to a final value F_f, thereby relating the fluorescence intensity F at a given time t with the pseudo-first-order rate constant k_{obs}. k_{obs} values obtained from this fit were plotted as a function of inhibitor concentration. The line through the data represents a fit to eq 6, from which second-order association rate constants were calculated.

different inhibitor concentrations and plotted as a function of [I]. A plot for compound **4** is shown in Figure 3B. A hyperbolic dependence of k_{obs} on the inhibitor concentration was detected that could be fit with eq 4. From this fit, we obtained $K_i = 24$ μM and $k_2 = 5 \times 10^{-3}$ s^{-1}. These values are in good agreement with those obtained from progress curve analysis (Table 1).

We next attempted to determine k_{-2}, the dissociation rate constant of the tight EI* complex. The dissociation kinetics of the four ketoacids turned out to be very slow and had to be followed for several days. Figure 4 shows the time-course of activity recovery for the complex between NS3 and compound **3**. The data were fit with a monophasic exponential equation to derive a value for the observed first-order rate constant of dissociation k_{off}. This rate constant is related to k_{-2} according to eq 8:

$$k_{off} = k_{-2}k_{-1}/(k_{-1} + k_2) \quad (8)$$

Under conditions of rapid equilibrium, $k_{-1} \gg k_2$ and k_{off} becomes a good approximation of k_{-2}. The dissociation rate constants of the EI* complex determined for compounds **3**, **4**, and **5** and estimated for compound **1** (see Materials and Methods) are listed in Table 1. The values are indicative of very tight complexes with complex half-lives of 11−48 h. The data allow the calculation of overall K_i* values according to eq 9:

$$K_i^* = K_i[k_{-2}/(k_{-2} + k_2)] \quad (9)$$

K_i* values for the tri- and tetrapeptides are in the low nanomolar range, whereas the hexapeptide has an overall $K_i^* = 10$ pM, the lowest value so far reported for an inhibitor of the NS3 protease.

The potential of generating very potent NS3 α-ketoacid inhibitors prompted us to gain more mechanistic insight into the interaction between the enzyme and this class of compounds. Ketoacids have the potential of transiently engaging in covalent bond formation between their α-carbonyl carbon and the O-γ of the catalytic serine residue. We have found that the fluorescent active site probe P binds with the same affinity to the wild-type NS3 protease and to its catalytic serine to alanine mutant (*51*). Figure 5 shows that ketoacid **3** displaces P from the wild type with an IC_{50} of 1.5 μM. A 73-fold higher concentration of compound was needed to displace the active site probe from the catalytic serine to alanine mutant (S139-A). Similar results were obtained with compounds **1** and **4**, providing a strong indication for the involvement of Ser 139 in the inhibition mechanism. A likely mechanistic explanation for the biphasic inhibition of the NS3 protease by α-ketoacids, in light of these findings, is the formation of a noncovalent collision complex in the first kinetic phase, followed by the much slower formation of a covalent bond between the catalytic serine hydroxyl and the α-carbonyl carbon of the inhibitor in the second phase. In principle, the K_i value of the collision complex, measured kinetically on the wild-type enzyme, should be comparable to the equilibrium dissociation constant extrapolated from the probe displacement on the S139-A mutant enzyme. Taking into account the probe concentration used in the assay and its K_d value, we estimated a dissociation constant of 36 μM for **3** on the mutant enzyme. Since this mutation was obtained in the context of the NS3 protease from the HCV Bk strain, we re-determined the K_i value for **3** on the Bk wild-type enzyme by progress curve analysis. The value thus obtained, 1 μM, was significantly lower than the value obtained in the binding assay on the mutant enzyme, suggesting that the serine to alanine mutation affects both phases of the reaction.

To gain kinetic evidence for the formation of a covalent bond in the second phase of the reaction, we took advantage of the fact that a proton transfer has to occur during the transition state of the hemiketal formation. If the microscopic process described by k_2 indeed corresponds to hemiketal formation, a solvent isotope effect (SIE) should be observable on this rate constant. Using **3,** we could indeed observe an

Table 1: Kinetic Parameters of the Inhibition of the NS3 Protease by Different α-Ketoacids[a]

compound	k_1 (M^{-1} s^{-1})	k_{-1} (s^{-1})	K_i (nM)	k_2 (s^{-1})	k_{-2} (s^{-1})	K_i* (nM)	$t/2$ (h)
1	6.5×10^7	0.2	4	2.3×10^{-3}	5.7×10^{-6}	0.01	34
3	nd	nd	4600	1.7×10^{-3}	4.0×10^{-6}	11	48
4	nd	nd	18500	5.0×10^{-3}	1.8×10^{-5}	67	11
5	nd	nd	17000	7.5×10^{-3}	1.2×10^{-5}	27	16

[a] Rate and equilibrium constants refer to the reactions outlined in mechanism B, Scheme 2. All data were determined in 50 mM Hepes, pH 7.5, 15% glycerol, 1 mM DTT, 1% CHAPS, and 80 μM Pep4AK containing varying concentrations of the NS3 protease domain, following the procedures described in the text. $t/2$ values were calculated from the values of k_{-2} according to $t/2 = \ln 2/k_{-2}$.

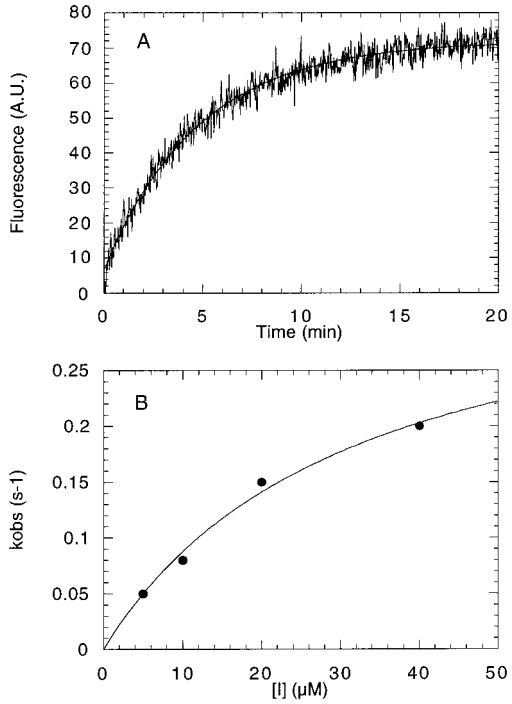

FIGURE 3: Protein fluorescence changes induced by addition of inhibitors to the NS3 protease. To 100 nM enzyme in 50 mM Hepes, pH 7.5, 1% CHAPS, 1 mM DTT, 15% glycerol, and 80 μM Pep4AK were added increasing amounts of **4**. Fluorescence was excited at 280 nm, and emission at 330 nm was continuously recorded. Panel A shows the fluorescence increase upon addition of 40 μM **4**. The fluorescence changes could be best fitted with the single-exponential equation: $F = F_0 + A[1 - \exp(-k_{obs}t)]$, describing the increase of the intrinsic protein fluorescence F_0 to a value $A + F_0$, occurring upon addition of the inhibitor, thereby relating the fluorescence intensity F at a given time t with the pseudo-first-order rate constant k_{obs}. Panel B: The observed pseudo-first-order rate constants obtained upon addition of increasing amounts of **4** were plotted as a function of inhibitor concentration. The line through the data represents a fit to eq 4 according to a biphasic mechanism with a slow step in the second phase (mechanism B in Scheme 2). Since very low values for the *y*-axis intercept were obtained, we fixed $k_{-2} = 1.8 \times 10^{-5}$ s^{-1}, the experimentally determined off-rate, for the fitting procedure.

SIE of 3.4 on the rate constant k_2 [$k_2(H_2O) = 1.7 \times 10^{-3}$ s^{-1} and $k_2(D_2O) = 5 \times 10^{-4}$ s^{-1}] whereas no significant SIE was determined on the K_i value of the initial complex [$K_i(H_2O) = 4.6$ μM and $K_i(D_2O) = 4.9$ μM]. This finding is indicative of k_2 describing an event that is rate-limited by a reaction step involving a proton transfer and suggestive of covalent bond formation occurring during the slow phase of the reaction.

The magnitudes of the rate constants k_1 and k_{-1}, indicative of fast equilibria, together with the absence of an SIE on the K_i value of the initial complex suggest that the latter reflects a noncovalent interaction between the ketoacids and

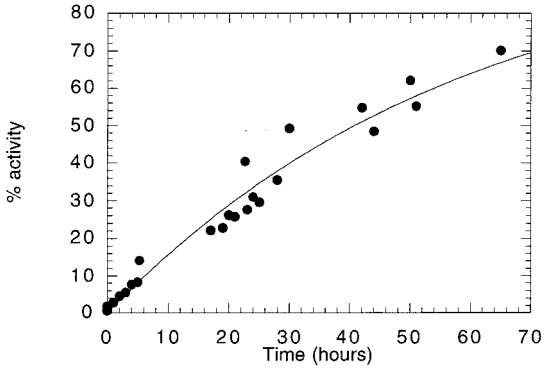

FIGURE 4: Dissociation kinetics of ketoacid **3** from its tight complex with the NS3 protease. Dissociation of the EI* complex was induced by dilution in the presence of 5 μM of the competitive inhibitor Ac-DEMEEC-OH ($K_i = 0.6$ μM) as a trapping agent as described under Materials and Methods. The recovery of enzymatic activity with time was monitored by incubating aliquots of the reaction mixture with 10 μM of substrate Ac-DED(Edans)EEAbuΨ[COO]-ASK(Dabcyl)-NH_2 and monitoring the extent of enzymatic cleavage of this substrate by HPLC. Data points obtained in 4 independent experiments are shown. The first-order dissociation rate constant was obtained from a fit of the data, shown by the line through the experimental data points, to the single-exponential equation: $A_t = A_f[1 - \exp(-k_{obs}t)]$, where A_t is the enzymatic activity expressed as a percentage of the activity of a control sample without inhibitor at a given time t, A_f is the extrapolated activity recovery at infinite time, and k_{obs} is the first-order rate constant associated with this process. From the fit, we obtained $A_f = 100$ and $k_{obs} = 0.015$ h^{-1}.

the active site of the NS3 protease. Remarkably, these noncovalent interactions allow for binding of the tetra- and tripeptide α-ketoacids **3**, **4**, and **5** whereas the corresponding α-carboxylic acids were inactive or very poorly active (*25*, *26*). This has induced us to characterize the initial EI complex in more detail, comparing its characteristics with the salient features of the interactions of the NS3 protease with hexapeptide α-carboxylic acids. We decided to explore three characteristic features of the inhibition of the NS3 protease by hexapeptide α-carboxylic acids: (1) Complex formation of α-carboxylic acids with the enzyme is crucially driven by electrostatic interactions, leading to an increase in K_i values with increasing ionic strength (*25*). (2) Binding of α-carboxylic acids involves the protonated catalytic histidine, resulting in increasing K_i values as a function of increasing pH (*23*). (3) The P1 α-carboxylate of hexapeptide acids was proposed to interact with the side chain of Lys 136, and mutation of this residue was shown to increase the K_i values of the compounds by about 1 order of magnitude (*23*). These characteristics were next compared to the behavior of α-ketoacids **1**, **3,** and **4**:

(1) Effect of ionic strength. Addition of 150 mM NaCl to the assay buffer increased the initial K_i value of **4** from 18.5 to 85 μM but had no significant effect on the rate constant k_2 (5×10^{-3} versus 6.6×10^{-3} s^{-1}).

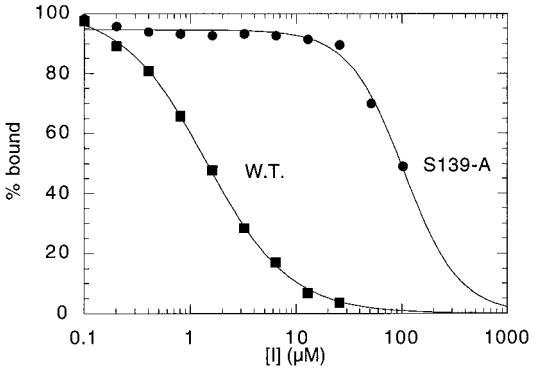

FIGURE 5: Interaction of ketoacid **3** with the S139A mutant of the NS3 protease. To 100 nM wild type or S139A mutant NS3 protease in 50 mM Hepes, pH 7.5, 2% CHAPS, 1 mM DTT, 50% glycerol, 80 μM Pep4AK, and 400 nM of the fluorescent active site probe Ac-D-E-Dap(*N*-β-dansyl)-E-Cha-C-OH were added increasing amounts of ketoacid **3**. At variance with all the other experiments, the NS3 protein (both wild type and mutant) from the HCV Bk strain was used. Displacement of the active site probe by compound **3** was measured as a decrease in fluorescence intensity at 510 nm upon excitation at 280 nm. All the measurements were made exactly after 5 min preincubation of the enzyme/probe complex with the ketoacid. The percent of displacement was plotted as a function of added inhibitor, and data were fitted with a two-parameter logistic equation to derive IC_{50} values of 1.5 and 110 μM for the wild type and mutant enzymes, respectively.

(2) pH dependence. The pH dependence of $1/K_i$ of **1** follows the ionizations in the free enzyme and the free inhibitor (*55*) and titrated with an apparent pK_a value of 6.9 (Figure 6A). Also, k_2 increased with increasing pH (Figure 6B). The pH dependence of this rate constant follows the ionization of the enzyme−inhibitor complex and titrated with an apparent p$K_a \geq 8.0$. Both pH−titration curves were noncooperative. In contrast, the pH dependence of K_i, following the ionizations in the enzyme−inhibitor complex, was highly cooperative, suggesting the involvement of multiple ionizable sites in its stabilization (Figure 6C).

(3) Effect of Lys 136. Mutation of Lys 136 into methionine had no significant effect on the initial K_i value of the complex between the NS3 protease and **3** (4.6 versus 5.5 μM). The mutation did, however, significantly affect the isomerization rate constant k_2 (1.7×10^{-3} versus 3×10^{-4} s^{-1}).

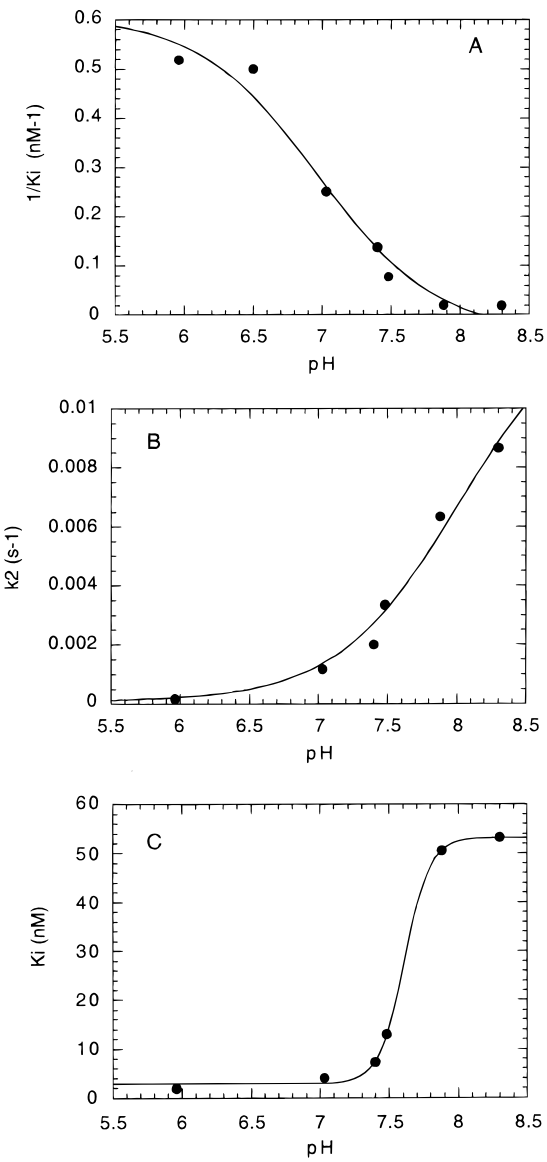

FIGURE 6: pH dependence of the inhibition of the NS3 protease by ketoacid **1**. Panels A−C: To 1 nM NS3 protease in 25 mM Tris, 12.3 mM acetate, 12.3 mM Mes, 15% glycerol, 1% CHAPS, 1 mM DTT, and 80 μM Pep4AK, pH 6.0−8.5, were added 10 μM of substrate Ac-DED(Edans)EEAbuΨ[COO]ASK(Dabcyl)-NH_2 together with increasing amounts of compound **1**. Families of progress curves were generated as described in the legend to Figure 1 and used to calculate K_i and k_2 values. The fractional occupancy of the enzyme's active site by the substrate was corrected for the pH dependence of its K_m value. pK_a values were calculated from a fit of the data to the equations $F(\text{pH}) = a + b10^{(\text{pH}-\text{p}K_a)}/[10^{(\text{pH}-\text{p}K_a)} + 1]$ or, with allowance for cooperativity, $F(\text{pH}) = a - [K^n/(K^n + 10^{-n(\text{pH})})](a - b)$, where F(pH) is the pH-dependent variable, a and b are the asymptotic values, and n is the Hill coefficient.

DISCUSSION

α-Ketoacids are slow-binding inhibitors of the hepatitis C virus NS3 protease. Their mechanism of interaction with the enzyme involves the rapid formation of a reaction intermediate that slowly interconverts into a tight complex. The presence of a kinetic intermediate on the reaction pathway was deduced from the hyperbolic dependence of the observed pseudo-first-order rate constants for the formation of the final enzyme−inhibitor complex on the inhibitor concentration and from the dependence of the initial velocities of progress curves on [I]. We interpret these data as a rapid formation of a noncovalent collision complex between the enzyme and the inhibitor that is followed by the slow formation of a covalent bond. The kinetics of the formation of the collision complex were characterized in detail for the hexapeptide α-ketoacid **1**, providing evidence for a very rapid equilibrium with the magnitude of the association rate constant being suggestive of a diffusion-limited encounter between the enzyme and the inhibitor. Figure 7 summarizes a possible reaction pathway that takes into account our experimental results. Electrostatic interactions are a dominant driving force for active site ligand recognition in the NS3 protease (*56*), and electrostatic calculations have shown that the protonated catalytic His 57 is a major contributor to the positive potential around the active site (Uwe Koch, unpublished observations). Accordingly, our model postulates the formation of a noncovalent complex in the first kinetic step in which, in addition to interactions involving the peptide portion of the molecule, an electrostatic stabilization occurs via the interaction of the ketoacid moiety with the protonated

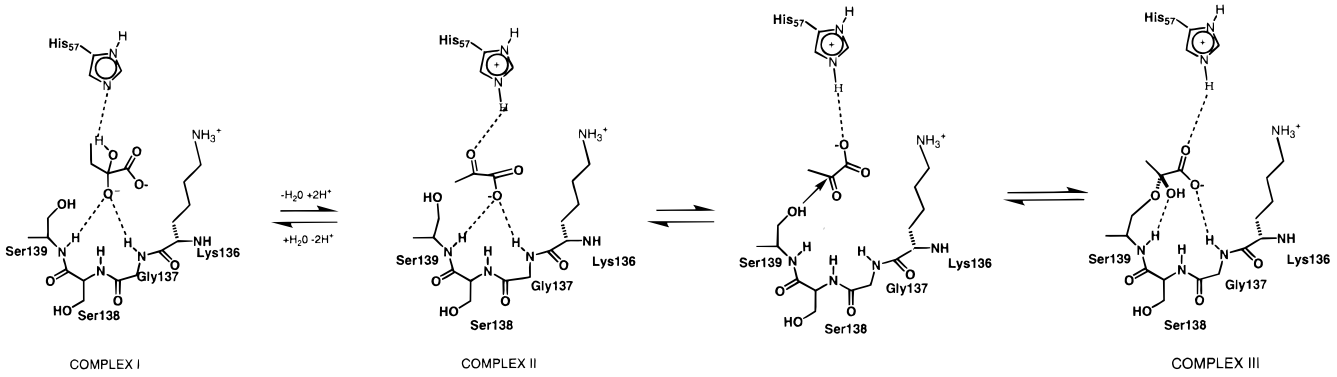

FIGURE 7: Possible pathway of inhibition of the NS3 protease by α-ketoacids. Interactions between the inhibitor and the active site of the protease were modeled based on experimental data obtained in this work and on the crystal structures of the complexes between p-APPA and trypsin (*38*) or thrombin (*39*). See text for details.

His 57. The experimental data that support this model are the following: (i) the magnitude of the association rate constant that suggests a diffusion-limited reaction; (ii) the ionic strength dependence of the initial K_i value, indicative of important electrostatic contributions to EI complex formation; and (iii) the pH dependence of $1/K_i$ that titrates with a p$K_a = 6.9$, a value that is similar to the pK_a value of His 57 (6.8) determined by NMR spectroscopy (*53*). Cooperativity in the pH dependence of K_i (Figure 6C) may arise from the fact that both the ionization of His 57 and the hydration of the ketoacid are pH-dependent phenomena. At low pH, complex II (Figure 7) should prevail, in which the ketoacid is bound in its ketone form, with the ketone being hydrogen-bonded to the protonated ϵ-N of His 57 and the carboxylic acid engaging in hydrogen bond interactions with the backbone amide of Gly 137. At higher pH, both deprotonation of His 57 and hydration of the ketone moiety of the inhibitor would be favored, possibly leading to complex I in Figure 7, where the hydrated ketone is hydrogen-bonded to the deprotonated ϵ-N of His 57 and an oxyanion is formed that is stabilized by hydrogen bonds to the amides of Gly 137 and Ser 139. Interconversion of the two forms could require the cooperative association of more than one proton, thereby possibly explaining the steepness of the titration curve.

Our mutagenesis data suggest that the binding mode of α-ketoacids in their initial complex differs substantially from that of peptide carboxylic acids. The affinity of the latter class of inhibitors was found to be significantly affected by mutagenesis of Lys 136 into methionine and was not influenced by the Ser 195 to alanine mutation (*23*, *51*). The contrary turned out to be true for α-ketoacids. The role of Ser 195 in the stabilization of the collision complex with α-ketoacids may be an indirect one. In fact, removal of the serine γ-OH in the mutant may alter the hydrogen bond network at the active site of the enzyme and thereby influence the correct positioning of His 57. Alternatively, the mutagenesis data may reflect the incipient formation of a covalent bond between the carbonyl carbon of the inhibitor and the Ser 139 γ-OH in complex II (Figure 7).

The covalent bond formation was proposed to occur in the second phase of the inhibition kinetics. This interpretation is based on (i) the pronounced stability (very low off-rates) of the EI* complex and (ii) the significant solvent isotope effect on the first-order rate constant of formation of this complex. It is instructive to compare the inhibition kinetics of the NS3 protease by peptide α-ketoacids with data obtained on the inhibition of thrombin or trypsin by *p*-amidinophenylpyruvate (p-APPA) (*37*). Whereas binding of the compound to thrombin was monophasic, a biphasic kinetic behavior, analogous to that reported herein, was observed for the reaction between trypsin and p-APPA. In the latter case, the rate constants k_2 and k_{-2}, describing the equilibrium between the initial complex and the covalent complex, have been determined as $k_2 = 3.15\ s^{-1}$ and $k_{-2} = 0.1\ s^{-1}$ (*37*). These data should be compared to $k_2 = 2.3 \times 10^{-3}\ s^{-1}$ and $k_{-2} = 5.7 \times 10^{-6}\ s^{-1}$ obtained for the complex between **1** and the NS3 protease, indicating a significantly larger energy barrier for both the formation and the dissociation of the covalent complex in the case of the NS3 protease. This remarkable difference has prompted us to investigate the nature of the rate-limiting step of covalent complex formation between α-ketoacids and NS3. We could show that complexation of NS3 with α-ketoacids goes along with protein fluorescence changes, suggestive of some conformational rearrangement. The solvent isotope effect on k_2, however, indicated that a chemical step rather than a conformational transition is likely to be the rate-limiting factor in tight complex formation. k_2 titrated with an apparent p$K_a \geq 8.0$. According to the reaction scheme in Figure 7, this pK_a value could possibly represent the pK_a value of His 57 in the noncovalent complex II. In fact, the noncovalently bound ketoacid is likely to perturb the pK_a value of His 57, stablizing its protonated form. Such pK_a perturbations of the catalytic histidine have been observed in complexes of chymotrypsin with trifluoromethyl ketones (*57*) or in subtilisin covalently modified with acidic groups positioned in the vicinity of the catalytic triad (*58*). Deprotonation of His 57 is required for this residue to act as a proton acceptor during hemiketal formation, which would explain the increase of k_2 with increasing pH.

Two pathways of formation of a covalent adduct are possible, depending on the stereochemistry of the nucleophilic attack of the ketoacid carbonyl carbon by the serine hydroxyl. X-ray crystal structures of p-APPA bound to trypsin (*38*) and thrombin (*39*) have provided evidence for attack from the *re*-side, leading to a type III complex (Figure 7) in these enzymes. This reaction pathway is kinetically favored since it implies the stabilization of the charged tetrahedral intermediate by the oxyanion hole of the enzyme. The striking difference between the kinetics of hemiketal formation in the p-APPA−trypsin complex compared to the

kinetics of covalent bond formation in the α-ketoacid−NS3 complexes could be indicative of structural differences of the final covalent complexes. This question will have to be addressed by X-ray crystallography or by NMR studies.

A comparison of the different kinetic data obtained with α-ketoacids **1**, **3**, **4**, and **5** indicates that the peptide length primarily determines the magnitude of the initial K_i value and has little effect on the rate constants k_2 and k_{-2}, describing the formation and dissociation of the covalent adduct. This is in line with the notion that these rate constants reflect chemical steps that predominantly depend on the nature of the ketoacid group. The overall potency of the compounds is clearly dictated by the extremely slow dissociation rate constant of the covalent adduct. This allows the generation of tripeptide inhibitors with overall potencies in the nanomolar range that may prove useful in the development of drug-like molecules aimed at inhibiting this enzyme in a physiological context.

ACKNOWLEDGMENT

We thank Raffaele Ingenito and Antonello Pessi for peptide synthesis and Stefania Orru' and Fabio Bonelli for mass spectrometry. We are grateful to Stefania Di Marco, Maurizio Sollazzo, Gaetano Barbato, Daniel Cicero, and Renzo Bazzo for many helpful discussions and for critical reading of the manuscript. We also thank Silvia Pesci for recording NMR spectra.

REFERENCES

1. Kim, J. L., Morgenstern, K. A., Lin, C., Fox, T., Dwyer, M. D., Landro, J. A., Chambers, S. P., Markland, W., Lepre, C. A., O'Malley, E. T., Harbeson, S. L., Rice, C. M., Murcko, M. A., Caron, P. R., and Thomson, J. A. (1996) *Cell 87*, 343−355.
2. Love, R. A., Parge, H. E., Wickersham, J. A., Hostomsky, Z., Habuka, N., Moomaw, E. W., Adachi, T., and Hostomska, Z. (1996) *Cell 87*, 331−342.
3. Yan, Y., Li, Y., Munshi, S., Sardana, V., Cole, J., Sardana, M., Steinkühler, C., Tomei, L., De Francesco, R., Kuo, L., and Chen, Z. (1998) *Protein Sci. 7*, 837−847.
4. Yao, N., Hesson, T., Cable, M., Hong, Z., Kwong, A. D., Le, H. V., and Weber, P. C. (1997) *Nat. Struct. Biol. 4*, 463−467.
5. Kim, J. L., Morgenstern, K. A., Griffith, J. P., Dwyer, M. D., Thomson, J. A., Murcko, M. A., Lin, C., and Caron, P. R., (1998) *Structure 6*, 89−100.
6. Lohmann, V., Koch, J. O., and Bartenschlager, R. (1996) *J. Hepatol. 24*, 11−19.
7. Urbani, A., De Francesco, R., and Steinkühler, C. (1999) in *Proteases of Infectious Agents* (Dunn, B., Ed.) pp 61−91, Academic Press, San Diego.
8. Yao, N., and Weber, P. (1998) *Antiviral Ther. 3*, 93−97.
9. Bartenschlager, R., Ahlborn-Laake, L., Mous, J., and Jacobsen, H. (1994) *J. Virol. 68*, 5045−5055.
10. Failla, C., Tomei, L., and De Francesco, R. (1994) *J. Virol. 68*, 3753−3760.
11. Lin, C., Thomson, J. A., and Rice, C. M. (1995) *J. Virol. 69*, 4373−4380.
12. Tanji, Y., Hijikata, M., Satoh, S., Kaneko, T., and Shimotohno, K. (1995) *J. Virol 69*, 1575−1580.
13. Steinkühler, C., Tomei, L., and De Francesco, R. (1996) *J. Biol. Chem. 271*, 6367−6373.
14. Shimizu, Y., Yamaji, K., Masuho, Y., Yokota, T., Inoue, H., Sudo, K., Satoh, S., and Shimotohno, K. (1996) *J. Virol. 70*, 127−132.
15. Steinkühler, C., Urbani, A., Tomei, L., Biasiol, G., Sardana, M., Bianchi, E., Pessi, A., and De Francesco, R. (1996) *J. Virol. 70*, 6694−6700.
16. Tomei, L., Failla, C., Vitale, R. L., Bianchi, E., and De Francesco, R. (1995) *J. Gen. Virol. 77*, 1065−1070.
17. Bianchi, E., Urbani, A., Biasiol, G., Brunetti, M., Pessi, A., De Francesco, R., and Steinkühler, C. (1997) *Biochemistry 36*, 7890−7897.
18. Urbani, A., Biasiol, G., Brunetti, M., Volpari, C., Di Marco, S., Sollazzo, M., Orru', S., Dal Piaz, F., Casbarra, A., Pucci, P., Nardi, C., Gallinari, P., De Francesco, R., and Steinkühler, C. (1999) *Biochemistry 38*, 5206−5215.
19. Barbato, G., Cicero, D., Nardi, C., Steinkühler, C., Cortese, R., De Francesco, R., and Bazzo, R. (1999) *J. Mol. Biol. 289*, 371−384.
20. Steinkühler, C., Urbani, A., Tomei, L., Biasiol, G., Sardana, M., Bianchi, E., Pessi, A., and De Francesco, R. (1996) *J. Virol. 70*, 6694−6700.
21. Urbani, A., Bianchi, E., Narjes, F., Tramontano, A., De Francesco, R., Steinkühler, C., and Pessi, A. (1997) *J. Biol. Chem. 272*, 9204−9209.
22. Zhang, R., Durkin, J., Windsor, W. T., McNemar, C., Ramanathan, L., and Le, H. V. (1997) *J. Virol. 71*, 6208−6213.
23. Steinkühler, C., Biasiol, G., Brunetti, M., Urbani, A., Koch, U., Cortese, R., Pessi, A., and De Francesco, R. (1998) *Biochemistry 37*, 8899−8905.
24. Llinas-Brunet, M., Bailey, M., Fazal, G., Goulet, S., Halmos, T., Laplante, S., Maurice, R., Poirer, M., Poupart, M. A., Thibeault, D., Wernic, D., and Lamarre, D. (1998) *Bioorg. Med. Chem. Lett. 8*, 1713−1718.
25. Ingallinella, P., Altamura, S., Bianchi, E., Taliani, M., Ingenito, R., Cortese, R., De Francesco, R., Steinkühler, C., and Pessi, A. (1998) *Biochemistry 37*, 8906−8914.
26. Cicero, D., Barbato, G., Koch, U., Ingallinella, P., Bianchi, E., Nardi, C., Steinkühler, C., Cortese, R., Matassa, V., De Francesco, R., Pessi, A., and Bazzo, R (1999) *J. Mol. Biol. 289*, 385−396.
27. La Plante, S. R., Cameron, D. R., Aubry, N., Lefebre, S., Kukolj, G., Maurice, R., Thibeault, D., Lamarre, D., and Llinas-Brunet, M (1999) *J. Biol. Chem. 274*, 18618−18624.
28. Stein, R. L., and Strimpler, A. M. (1987) *Biochemistry 26*, 2611−2615.
29. Shah, D., Lai, K., and Gorenstein, D. G. (1984) *J. Am. Chem. Soc. 106*, 4272−4273.
30. Imperiali, B., and Abeles, R. H. (1986) *Biochemistry 25*, 3760−3767.
31. Stein, R. L., Strimpler, A. M., Edwards, P. D., Lewis, J. J., Mauger, R. C., Schwarz, J. A., Stein, M. M., Trainor, D. A., Wildonger, R. A., and Zottola, M. (1987) *Biochemistry 26*, 2682−2689.
32. Brady, K., and Abeles, R. H. (1990) *Biochemistry 29*, 7608−7617.
33. Brady, K., Wei, A., Ringe, D., and Abeles, R. H. (1990) *Biochemistry 29*, 7600−7607.
34. Angelastro, M. R., Baugh, L. E., Bey, P., Burkhart, J. P., Chen, T. M., Durham, S. L., Hare, C. M., Huber, E. W., Janusz, M. J., Koehl, J. R., Marquart, A. L., Mehdi, S., and Peet, N. P. (1994) *J. Med. Chem. 37*, 4538−4554.
35. Brady, S. F., Sisko, J. T., Stauffer, K. J., Colton, C. D., Qiu, H., Lewis, S. D., Ng, A. S., Shafer, J. A., Bogusky, M. J., Veber, D. F., and Nutt, R. F. (1995) *Bioorg. Med. Chem. 3*, 1063−1078.
36. Bachovchin, W. W., Wong, W. Y. L., Farr-Jones, S., Shenvi, A. B., and Kettner, C. A. (1988) *Biochemistry 27*, 7689−7697.
37. Tanizawa, K., Kanaoka, Y., Wos, J. D., and Lawson, W. (1985) *Biol. Chem. Hoppe-Seyler 366*, 871−878.
38. Walter, J., and Bode, W. (1983) *Hoppe-Seyler's Z. Physiol. Chem. 364*, 949−959.
39. Chen, Z., Li, Y., Mulichak, A. M., Lewis, S., and Shafer, J. A. (1995) *Arch. Biochem. Biophys. 322*, 198−203.
40. Landro, J., Raybuck, S., Luong, Y. P. C., O'Malley, E. T., Harbeson, S. L., Morgenstern, K. A., Rao, G., and Livingston, D. J. (1997) *Biochemistry 36*, 9340−9348.
41. Llinas-Brunet, M., Bailey, M., Deziel, R., Fazal, G., Gorys, V., Goulet, S., Halmos, T., Maurice, R., Poirer, M., Poupart,

M. A., Rancourt, J., Thibeault, D., Wernic, D., and Lamarre, D. (1998) *Bioorg. Med. Chem. Lett. 8*, 2719−2724.
42. Narjes, F., Koehler, K., Steinkühler, C., Brunetti, M., Altamura, S., De Francesco, R., Pessi, A., Koch, U., and Matassa, V. G. A (1999), submitted for publication.
43. Hoeg-Jensen, T., Jakobsen, M. H., and Holm, A. (1991) *Tetrahedron Lett. 32*, 6387.
44. Bodanszky, M. (1993) *Peptide Chemistry*, 2nd revised ed., Springer-Verlag, Berlin.
45. De Francesco, R., Urbani, A., Nardi, M. C., Tomei, L., Steinkühler, C., and Tramontano, A. (1996) *Biochemistry 35*, 13282−13287.
46. Taliani, M., Bianchi, E., Narjes, F., Fossatelli, M., Urbani, A., Steinkühler, C., De Francesco, R., and Pessi, A. (1996) *Anal. Biochem. 240*, 60−67.
47. Cerretani, M., Di Renzo, L., Serafini, S., Vitelli, A., Gennari, N., Bianchi, E., Pessi, A., Urbani, A., Colloca, S., De Francesco, R., Steinkühler, C., and Altamura, S. (1999) *Anal. Biochem. 266*, 192−197.
48. Williams, J. W., and Morrison, J. F. (1979) *Methods Enzymol. 63*, 437−467.
49. Morrison, J. F. (1982) *Trends Biochem. Sci. 7*, 102−105.
50. Cha, S. (1976) *Biochem. Pharmacol. 25*, 2695−2702.
51. Fattori, D., Urbani, A., Brunetti, M., Ingenito, R., Pessi, A., Prendergast, K., Narjes, F., Matassa, V. G., De Francesco, R., and Steinkühler, C. (2000) *J. Biol. Chem.* (in press).
52. Schowen, K. B., and Showen, R. L. (1982) *Methods Enzymol. 87*, 551−606.
53. Urbani, A., Bazzo, R., Nardi, M. C., Cicero, D. O., De Francesco, R., Steinkühler, C., and Barbato, G. (1998) *J. Biol. Chem.* 273, 18760−18769.
54. Lewis, S. D., Lucas, B. J., Brady, S. F., Sisko, J. T., Cutrona, K. J., Sanderson, P. E., Freidinger, R. M., Mao, S. S., Gardell, S. J., and Shafer, J. A. (1998) *J. Biol. Chem. 27*, 273, 4843−4854.
55. Fersht, A. (1985) *Enzyme Structure and Mechanism*, Freeman and Co., New York.
56. Koch, U, Steinkühler, C., Cicero, D., Prendergast, K., Matassa, V. G., and Pessi, A. (1999), submitted for publication.
57. Lin, J., Cassidy, C. S., and Frey, P. (1998) *Biochemistry 37*, 11940−11948.
58. DeSantis, G., and Jones, J. B. (1998) *J. Am. Chem. Soc. 120*, 8582−8586.

BI9924260